LTNE approach to simulate temperature of cathode in a PEMFC

Khan, Munir; Yuan, Jinliang; Sundén, Bengt

2009

LTNE approach to simulate temperature of cathode in a PEMFC

Munir Ahmed Khan, Jinliang Yuan, Bengt Sundén

Munir.khan@energy.lth.se, Jinlian.Yuan@energy.lth.se, Bengt.Sunden@energy.lth.se

Department of Energy Sciences, Faculty of Engineering

Lund University, Box 118, SE-221 00 Lund, Sweden

Ph: +46-46-2228604, Fax:+46-46-2224717

Abstract

The solid phase and fluid phase temperature and species distribution have been calculated numerically in this study. The model considered here consists of catalyst layer, porous-transport layer and the current collector region (rib). Two energy equations approach has been employed in the porous transport layer and one energy equation is solved for the catalyst layer to simulate the temperature distribution. Full multi-component diffusion model and Knudsen effect have been included for the simulation of the species distribution in both catalyst and porous-transport layer. The agglomerate model has been used to simulate the catalyst layer. It has been found that the diffusion coefficient is low in the catalyst layer due to low permeability and porosity causing stagnation zones and the temperature rise is maximum in the stagnation zones causing local hot spots.

Keywords: Numerical study; Two equation energy approach; Agglomerate Model; Diffusion Coefficient; Stagnation Zones

1. Introduction

Polymer electrolyte membrane fuel cells (PEMFCs) have attained a considerable amount of attention in the research society in the last decade for their habit as environment friendly and high efficiency energy production units for both mobile and stationary units. Only few hurdles need to be overcome before PEMFCs can be launched in full commercial scale. One of the major hurdles still faced by the PEMFCs is their water management. PEMFCs use a solid polymer like SOFCs which give these two a major advantage over other fuel cell counterparts because of their stability. But, in PEMFCs, the ionic conductivity of the electrolyte is strongly dependant on the water content; more water content means higher conductivity. So, it is imperative for electrolyte to be damped at all times. On the

other hand, high water content in the cell can choke the flow of oxidant to the reaction site causing shutting down of the system. In order for the PEMFCs to work, a good water balance has to be maintained in the cell [1]. In conjunction to the above stated balance, thermal distribution in the cell plays a vital role in balancing the water content while the inlet supply is pre-humidified.

Since practical measurements are difficult to perform inside the fuel cell due to its compact nature and in order to visualize the internal behavior and response of the cell to the operating conditions, numerical simulations are mostly relied upon and in order to achieve reliable and accurate results, catalyst layer has been the main focus of interest because of the electro-chemical reactions occurring in it [2]. Up till now, many different approaches have been applied to simulate the catalyst layer where the agglomerate model has produced more explanatory results of the actual behavior of a PEMFC [2-5].

In this study, the transport phenomenon has been studied in depth for simulating the temperature distribution in the cathode side of a low pressure operating PEMFC. Since PEMFCs are low temperature operating devices, i.e., the temperature difference between the inlet and outlet is very low, thus a low temperature difference between the solid and fluid phase cause significant local thermal non-equilibrium (LTNE) [6]. Then separate energy equations are employed for the solid and fluid phases with inter transfer of energy among them.

2. Numerical models and equations

A schematic drawing of a typical porous cathode in contact with an interdigitated flow field of a PEMFC is given in Figure 1. The present computation is limited to a repeated section between the inlet and outlet channel.

The air-water vapor mixture enters into the porous cathode from the section inlet and transverses the porous transport layer (PTL) to the catalyst layer. The oxygen reduction reaction occurring in the catalyst layer consumes oxygen and, meanwhile produces water vapor. It can be presented as;

$$O_2 + 4H^+ + 4e^- \longleftrightarrow 2H_2O \qquad (1)$$

During the reaction, heat due to overpotential and irreversibility is generated. It should be removed from the cathode by the fluids or the solid.

Model Assumptions

The following assumptions have been made in the present model;

1. The cell is operating at steady conditions.
2. Inlet mixture is modeled as ideal and laminar flow.
3. The PTL is composed of void spaces and carbon fibers.
4. The catalyst layer is composed of agglomerate made of platinum particles supported by carbon and ionomer electrolyte.

5. The inlet and current collector temperature is uniform.

6. Water exits as gas only.

Governing Equations

In both catalyst and porous transport layers, the steady volume averaged continuity and momentum equations are solved, i.e.,

$$\nabla\left(\rho \cdot u_{Darcy}\right) = S_1 \qquad (2)$$

and,

$$\rho_f u \cdot \nabla u = -\nabla p + \nabla \cdot (\mu \nabla u) + S_2 \qquad (3)$$

The source term in (2) denotes the increase and decrease in the mass flow rate of the species due to chemical reactions occruing in the catalyst layer and back flow and osmotic drag of water to and from the membrane. The source term in (3) accounts for the viscous loss term as given in Table 1.

The species transport in the present study is handled by the general transport equation given by

$$\nabla \cdot \left(\rho u X_A\right) = -\nabla \cdot J_A + S_3 \qquad (4)$$

where J_A is the diffusion flux for a species *i* and is given by

$$J_A = -\rho D_{A,eff} \nabla X_A \qquad (5)$$

The diffusion coefficient $D_{A,gm}$ of a particular species in (5) can be calculated based on the binary diffusion coefficients in the multi-component gas mixture [7, 8].

$$D_{A,gm} = \frac{1 - Y_A}{Y_B / D_{AB} + Y_C / D_{AC} + \cdots} \qquad (6)$$

Since the catalyst layer and the PTL are both porous media, Knudsen diffusion is an active phenomenon in the porous media and needs to be also accounted in the model [9].

$$D_{i,k} = \frac{2}{3} r_e v_i = \frac{2}{3} r_e \sqrt{\left(\frac{8RT}{\pi M_i}\right)} \qquad (8)$$

In the present model an effective diffusion coefficient has been estimated based on both molecular and Knudsen diffusion given as [7];

$$D_{i,eff} = \varepsilon^{\tau}\left(\frac{D_{i,gm} \times D_{i,k}}{D_{i,gm} + D_{i,k}}\right) \qquad (9)$$

The temperatures in both the solid and fluid phases in the catalyst layer and PTL are modeled by applying the energy equation. The effective thermal conductivity of both phases is calculated as [5, 6, 8, 10];

$$k_{f,eff} = \varepsilon k_f \quad (10)$$

and,

$$k_{s,eff} = (1-\varepsilon)k_s \quad (11)$$

Since the chemical reactions are taking place in the catalyst layer, so the energy equation in the catalyst layer employs a source term for heat generation.

$$(\rho c_P)u \cdot \nabla T_f = \nabla \cdot (k_{f,eff} \nabla T_f) + S_4 \quad (12)$$

For the solid media, the energy equation is given as;

$$0 = \nabla \cdot (k_{s,eff} \nabla T_f) + S_5 \quad (13)$$

In the PEMFCs, the electrochemical reactions occur at the interface of the platinum catalyst surface and the fluid. Hence both the phases in the catalyst layer are assumed to be at the same temperature [6, 11, 12] i.e.;

$$T_f = T_s \quad (14)$$

Because two energy equations are solved for the porous transport layer, there is an inter-transfer of energy between the two phases as given in Table 1. The value of the interstitial heat transfer coefficient for the present case has been selected as 1.0×10^6 W·m^{-3}·K^{-1} [6].

Source Terms

All the governing equations, as described in the previous sections, remain the same for all type of catalyst layer models except for the source terms that are utilized to account for different species transport and reaction mechanism. In the agglomerate model, oxygen travels to the surface of the agglomerate and dissolves into the electrolyte phase. Once oxygen has been dissolved into the electrolyte, it is transported through the electrolyte film which has engulfed the agglomerate.

In order to describe the agglomerate catalyst model, standard Butler-Volmer kinetics can be utilized as [13];

$$i = a_{Pt}^{eff} i_o \frac{C_{O_2}}{C_{O_2}^{reff}} \left[\exp\left(-\frac{a_c F}{RT} \eta_{act} \right) - \exp\left(\frac{(1-a_c)F}{RT} \eta_{act} \right) \right] \quad (15)$$

For numerical simulations applications, the above equation can be arranged as [4, 5];

$$\nabla \cdot i = 4F \frac{p_{tot} X_{O_2}}{H_{O_2-N}} \left(\frac{1}{E_r k_c (1-\varepsilon_c)} + \frac{(r_{agg} + \delta_{agg})\delta_{agg}}{a_{agg} r_{agg} D_{O_2,N}} \right)^{-1} \quad (16)$$

where H_{O_2-N} is Henry's constant which represents the solubility of oxygen into Nafion, and it can be estimated as [1];

$$H_{O_2-N} = 1.33\times10^{-6} \exp\left(\frac{-498}{T} \right) \times p \quad (17)$$

E_r is the effectiveness factor and for the spherical agglomerate as used in the present model, it is given by [4, 5];

$$E_r = \frac{1}{\Phi_L}\left(\frac{1}{\tanh(3\Phi_L)} - \frac{1}{3\Phi_L}\right) \quad (18)$$

Thiele's modulus for a spherical agglomerate, ϕ_L , and estimated by [4, 5];

$$\Phi_L = \frac{r_{agg}}{3}\sqrt{\frac{k_c}{D_{eff}}} \quad (19)$$

D_{eff} represents the diffusion of oxygen into Nafion and can be correlated using [1];

$$D_{eff} = \left(0.0031 \times 10^{-4}\left(-\frac{2768}{T}\right)\right) \times \phi_{agg}^{1.5} \quad (20)$$

The reaction rate constant k_c, is [4, 5, 14] ;

$$k_c = \left(\frac{a_{Pt}^{agg}}{zF\,(1-\varepsilon_c)}\right)\left(\frac{i_o}{C_{O_2}^{reff}}\right)\left[\exp\left(-\frac{a_c F}{RT}\eta_{act}\right) - \exp\left(-\frac{(1-a_c)F}{RT}\eta_{act}\right)\right] \quad (21)$$

The exchange current density i_0 is obtained by temperature corrected relation given as

$$i_0 = i_0^{ref} \exp\left[-\frac{E_{act}}{R}\left(\frac{1}{T} - \frac{1}{T_0}\right)\right] \quad (22)$$

On the basis of the above discussed agglomerate catalyst model, the source terms for different governing equations are summarized in Table 1. Table 2 gives the values for the model and kinetic parameters used in the current simulation.

The source term for the water flux accounts for electro-osmotic drag and back diffusion. The convection of the water vapors from membrane towards cathode due to the pressure gradient that arises due to capillary pressure and elastic stresses have been ignored in the current model.

3. Numerical Methods

For the present case, due to high inter dependency of species and temperature distribution along the domain, all the governing equations have been coupled and solved using 3rd order discretization with convergence criteria set to 10^{-6}. Grid independence was achieved at 220×514 uniform control volumes due to the simple case geometry. The inlet of the domain is treated as a pressure inlet while the interface between the catalyst layer and membrane is set as an adiabatic wall by assuming that there is no transfer of energy over this interface. The inlet temperature of the fluid phase and the temperature of the current collector have been fixed at a steady value of 340K.

4. Results and Discussion

The velocity distribution for the cathode side is shown in Figure 2. Velocity is minimal in the catalyst layer due to lower permeability of the catalyst layer. Within the PTL, the velocity is comparatively higher in the region near the current collector because of the shorter flow path. Stagnation zones are created in the upper and lower left corners of the domain causing temperature rise being maximum as heat conduction remains the only mode of heat transfer.

In the cathode side, pre-humidified air (O_2, H_2O and N_2) with mass fractions of 0.2284, 0.0198 and 0.7518 enters into the domain and transverses through both the porous transport and catalyst layers. In the catalyst layer oxidation reduction reactions occur as given in Eq. (1). The reaction rate is dependant on quite many parameters including both physical and operating parameters. The physical parameters are accounted for by using the agglomerate model.

Initially the oxygen concentration is high, hence the chemical reaction rate is large but as the mixture transverses the domains the reaction rate decreases and becomes small due to consumption of oxygen. Since, in the catalyst layer, the reaction rate is highly dependent on the presence of oxygen in the domain, so in the present study a multi-component diffusion model is used for in-depth distribution analysis including the Knudsen diffusion. For density and specific heat capacity calculations, the volume-weighted mixing law has been incorporated. The numerical result of the species distribution is shown in Figure 3.

Figure 4 shows the temperature distribution inside the cathode of a PEMFC. In the catalyst layer, since the electro-chemical reactions are assumed to occur at the interface of the solid and fluid phase, the fluid and solid phases are considered to have same temperature [6, 11, 12]. In PTL, a two-equation model has been incorporated by employing separate energy equations for the solid and fluid phases with inter transfer of energy. The temperature of the solid phase in PTL is lower than the fluid phase because the solid has higher thermal conductivity. At the inlet, the fluid enters the domain with a uniform temperature and is heated up due to transfer of energy from the solid phase, whereas, the solid phase is cooled by the fresh inlet fluid. Near the exit of the domain, the fluid phase is at higher temperature than the solid phase due to the chemical reactions occurring in the catalyst layer. The solid phase is then heated up by the fluid phase.

5. Conclusion

In the present study, the cathode side of a low pressure PEMFC has been simulated using an agglomerate and two equation thermal model at high operating voltage. For species distribution, a multi-component diffusion model has been incorporated where density and specific heat capacity has been calculated by volume-weighted mixing law. All the parameters are strongly temperature dependent while the reaction rate is coupled with the distribution of species within the domain. It has been observed that higher temperature leads to higher reaction rates but the oxidant concentration limits the rise due to the decrease in concentration as the mixture transverses towards the module outlet. The diffusion coefficient is minimum in the catalyst layer due to the low porosity and permeability.

Stagnation zones are created in the catalyst layer leading to which local hot spots where heat conduction is the primary cooling phenomenon.

5. Nomenclature

a_{agg}	Effective agglomerate surface area ($m^2 \cdot m^{-3}$)
a_{Pt}^{eff}	Effective catalyst surface area ($m^2 \cdot m^{-3}$)
a_c	Cathodic transfer coefficient
c_p	Specific heat capacity ($J \cdot kg^{-1} \cdot K^{-1}$)
$C_{O_2}^{ref}$	Reference O_2 concentration ($mol \cdot m^{-3}$)
$D_{i,eff}$	Effective diffusivity of species i ($m^2 \cdot s^{-1}$)
$D_{A,gm}$	Binary diffusion coefficient of species in mixture ($m^2 \cdot s^{-1}$)
D_{eff}	Effective diffusivity of dissolved oxygen in electrolyte ($m^2 \cdot s^{-1}$)
F	Faraday's constant
H	Henry's constant ($Pa \cdot m^3 \cdot mol^{-1}$)
h_v	Interstitial heat transfer coefficient ($W \cdot m^{-3} \cdot K^{-1}$)
k_c	Reaction rate constant (s^{-1})
i	Current density ($A \cdot m^{-2}$)
i_o	Local exchange current density ($A \cdot m^{-2}$)
M	Molecular weight of gas mixture ($kg \cdot mol^{-1}$)
M_i	Molecular weight of species ($kg \cdot mol^{-1}$)
m_{Pt}	Platinum loading ($kg \cdot m^{-2}$)
u	Velocity vector ($m \cdot s^{-1}$)
p	Pressure (Pascals)
r_{agg}	Radius of agglomerate (m)

R	Universal gas constant ($J \cdot mol^{-1} \cdot K^{-1}$)
X	Species mass fraction
Y	Species molar fraction
z	Number of electrons consumed per mole of reactant

Greek Letters

α	Net drag coefficient of water molecule per proton
δ_{agg}	Thickness of electrolyte film covering an agglomerate (m)
ε_{agg}	Proportion of electrolyte in agglomerate
ε	Porosity of material
ε_c	Porosity of catalyst layer
Φ_L	Theile's modulus
η_{act}	Local activation overpotential (V)
ρ	Density ($kg \cdot m^{-3}$)

Subscripts and superscripts

agg	Agglomerate
c	Catalyst layer
eff	Effective
f	Fluid phase
i	Species
Pt	Platinum
s	Solid phase

6. Acknowledgement

The Swedish Research Council (VR) partially supported the current research. The first author thanks the financial support of his Ph.D. study from Higher Education Commission, Pakistan, administered by the Swedish Institute (SI).

7. References

1. Chang, S.-M. and H.-S. Chu, *A transient model of PEM fuel cells based on a spherical thin film-agglomerate approach.* J. Power Sources, 2007. **172**: p. 790-798.
2. Siegel, N.P., et al., *Single domain PEMFC model based on agglomerate catalyst geometry.* J. Power Sources, 2003. **115**(1): p. 81-89.
3. Broka, K. and P. Ekdunge, *Modelling the PEM fuel cell cathode.* J. Appl. Electrochem, 1997. **27**: p. 281-89.
4. Harvey, D., J.G. Pharoah, and K. Karan, *A comparison of different approached to modeling the PEMFC catalyst layer.* J. Power Sources, 2008. **179**: p. 209-19.
5. Sun, W., B.A. Peppley, and K. Karan, *An improved two-dimensional agglomerate cathode model to study the influence of catalyst layer structural parameters.* Electrochem. Acta, 2005. **50**(16-17): p. 3359-74.
6. Hwang, J.J. and Chen. P.Y., *Heat/mass transfer in porous electrodes of fuel cells.* Intl. J. Heat and Mass Transfer, 2006. **49**: p. 2315-27.
7. Haberman, B.A. and J.B. Young, *Three-dimensional simulation of chemically reacting gas flows in the porous support structure of an integrated-planar solid oxide fuel cell.* Intl. J. Heat and Mass Transfer, 2004. **47**: p. 3617-29.
8. Yuan, Jinliang, XinRong Lv, Bengt Sunden, Dantin Yue , *Analysis of parameter effects on the transport phenomena in conjunction with chemical reactoins in ducts relevant for methane reformers.* Intl. J. Hydrogen Energy, 2007. **32**: p. 3887-98.
9. Reid, C.R., J.M. Prausnitz, and P.B. E., *The properties of gases & liquids*. 4th ed. 1986, New York: McGraw-Hill Book Company.
10. *Fluent user's guide*: Fluent Inc.
11. Hwang, A.J.J., *A complete two-phase model of a porous cathode of a PEM fuel cell.* J. Power Sources, 2007. **164**: p. 174-81.
12. Hwang, A.J.J., et al., *Modeling of two-phase temperature in a two-layer porous cathode of polymer electrolyte fuel cells.* Intl. J. Hydrogen Energy, 2007. **32**: p. 405-14.
13. Bard, A.J. and F. L.R., *Electrochemical methods-Fundamentals and Applications*. 2nd ed. 2001, New York: John Wiley & Sons Inc.
14. Gallart, M.S., *Computational modeling and optimization of proton exchange membrane fuel cells*, in *Mechanical Engineering*. 2007, University of Victoria.

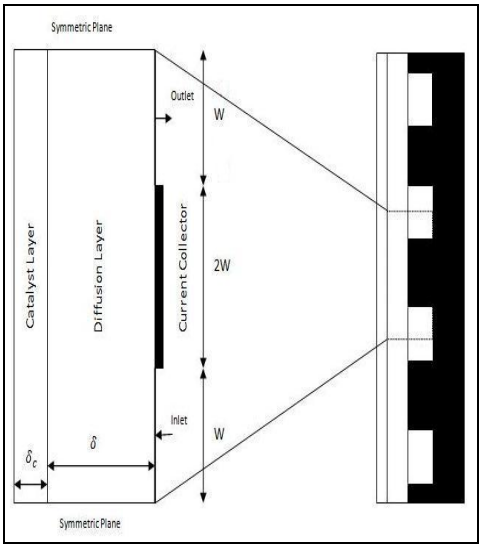

Figure 1: Schematic drawing of a porous electrode of the interdigitated flow field

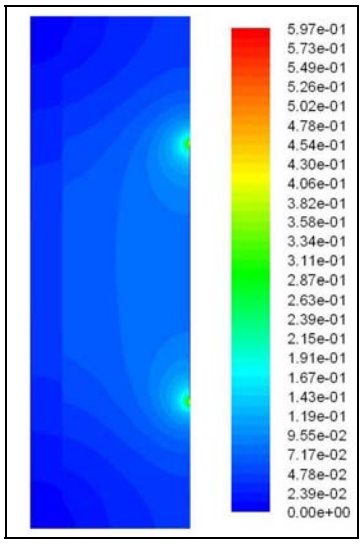

Figure 2: Velocity magnitude distribution pattern in cathode of PEMFC (m/s)

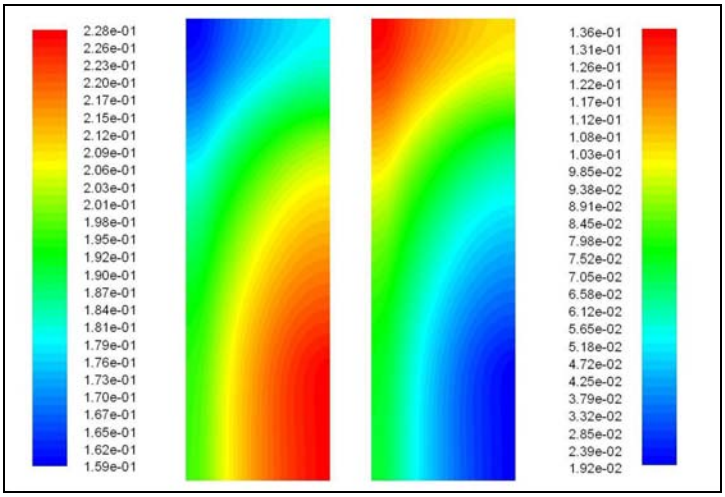

Figure 3: Mass fraction distribution in the cathode of PEMFC: (Left) O_2; (Right) H_2O

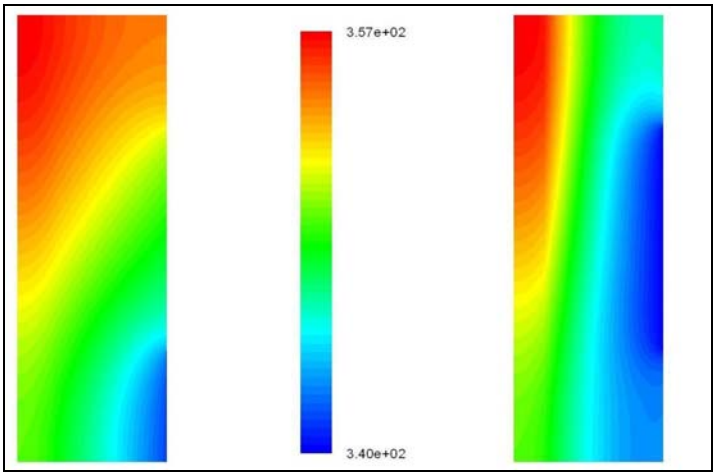

Figure 4: Temperature (K) distribution inside cathode of a PEMFC:(Left) Fluid Phase; (Right) Solid Phase

Table 1: Source terms based on agglomerate model

	Source terms	
	Catalyst Layer	Porous Transport Layer
Mass	$-\frac{M_{O_2}}{4F}\nabla\cdot i+\frac{M_{H_2O}}{2F}\nabla\cdot i+\frac{\alpha M_{H_2O}}{F}\nabla\cdot i$	0
Momentum	$S_{2,1}=-(\mu D_c u)$	$S_{2,1}=-(\mu D_{PTL} u)$
Species	$-\frac{M_{O_2}}{4F}\nabla\cdot i+\frac{M_{H_2O}}{2F}\nabla\cdot i+\frac{\alpha M_{H_2O}}{F}\nabla\cdot i$	0
Energy (Fluid)	$\eta(\nabla\cdot i)$	$h_v(T_s-T_f)$
Energy (Solid)	$T_s=T_f$	$-h_v(T_s-T_f)$

Table 2: Physical and kinetic parameters used in current model*

Thermo-Physical Properties	Density (solid)	1100 $kg.m^{-3}$
	Thermal conductivity (solid)	1.71 $Wm^{-2}K^{-1}$
	Thermal conductivity (fluid)	0.051 $Wm^{-2}K^{-1}$
	Viscosity	$1.5863x10^{-5}$ m^2s^{-1}
	Interstitial heat transfer coefficient	10^6 $W.m^{-3}.K^{-1}$
	Stiochiometric flow ratio	5.0
Geometric Properties	GDL Porosity	48%
	CL Porosity	42%
	CL Viscous Resistance	$9.775x10^{11}$ m^{-2}
	GDL Viscous Resistance	$6.537x10^{11}$ m^{-2}

	Surface to volume ratio	1000 m^{-1}
Agglomerate Properties	Platinum loading	4 $g.m^{-3}$
	Platinum radius	1.5 nm
	Agglomerate radius	1 µm
	Effective agglomerate area	$3.6x10^{5}$ $m^{2}m^{-3}$
	Reference exchange current density	$3.85x10^{-8}$ $A.cm^{-2}$
	Activation energy	$76.5x10^{3}$ $J.mol^{-1}$
	Charge transfer coefficient	1
	Reference O_2 Concentration	3.6551 $mol.m^{-3}$
	Effective Pt surface ratio	0.75
	* [1, 3-5, 11, 14]	